The force control and path planning of electromagnetic induction-based massage robot

Wendong Wang*, Lei Zhang, Jinzhe Li, Xiaoqing Yuan, Yikai Shi, Qinqin Jiang and Lijing He
School of Mechanical Engineering, Northwestern Polytechnical University, Xi'an, Shaanxi, China

Abstract.
BACKGROUND: Massage robot is considered as an effective physiological treatment to relieve fatigue, improve blood circulation, relax muscle tone, etc. The simple massage equipment quickly spread into market due to low cost, but they are not widely accepted due to restricted massage function. Complicated structure and high cost caused difficulties for developing multi-function massage equipment.
OBJECTIVE: This paper presents a novel massage robot which can achieve tapping, rolling, kneading and other massage operations, and proposes an improved reciprocating path planning algorithm to improve massage effect.
METHODS: The number of coil turns, the coil current and the distance between massage head and yoke were chosen to investigate the influence on massage force by finite element method. The control system model of the wheeled massage robot was established, including control subsystem of the motor, path algorithm control subsystem, parameter module of the massage robot and virtual reality interface module. The improved reciprocating path planning algorithm was proposed to improve regional coverage rate and massage effect.
RESULTS: The influence caused by coil current, the number of coil turns and the distance between massage head and yoke were simulated in Maxwell. It indicated that coil current has more important influence compared to the other two factors. The path planning simulation of the massage robot was completed in Matlab, and the results show that the improved reciprocating path planning algorithm achieved higher coverage rate than the traditional algorithm.
CONCLUSIONS: With the analysis of simulation results, it can be concluded that the number of coil turns and the distance between the moving iron core and the yoke could be determined prior to coil current, and the force can be controllable by optimizing structure parameters of massage head and adjusting coil current. Meanwhile, it demonstrates that the proposed algorithm could effectively improve path coverage rate during massage operations, therefore the massage effect can be improved.

Keywords: Massage robot, electromagnetic induction, massage force, path planning, coverage rate

1. Introduction

Massage equipment can effectively alleviate the shortage of masseur/masseuse, and help to improve the quality of life for the elderly or those who are suffering from bone/muscle diseases [1,2]. The existing massage apparatuses, which act like a human hand to perform massage operations by mechanical tool, airbags and electric device to promote blood circulation and eliminate muscle fatigue [3,4]. All over the world many research institutes made efforts to improve massage effect [5,6].

*Corresponding author: Wendong Wang, School of Mechanical Engineering, Northwestern Polytechnical University, 127 West Youyi Road, Xi'an 710072, Shaanxi, China. Tel.: +86 02988494893; E-mail: wdwang@nwpu.edu.cn.
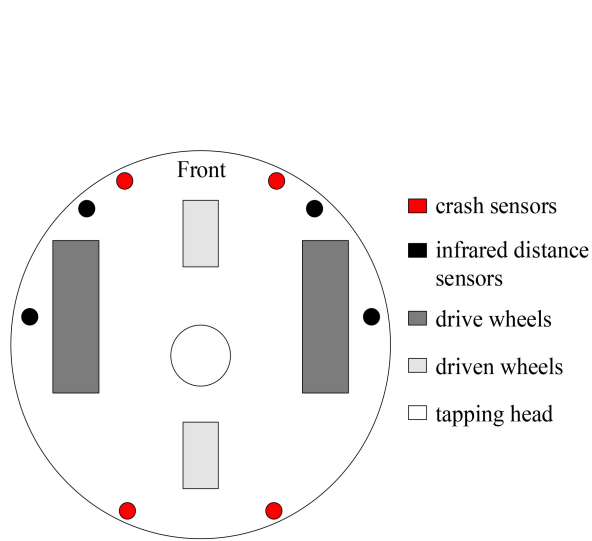
Front

- ■ crash sensors
- ■ infrared distance sensors
- ■ drive wheels
- ☐ driven wheels
- ☐ tapping head

Fig. 1. Schematic configuration of massage robot.

connection rod

moving iron corn

yoke

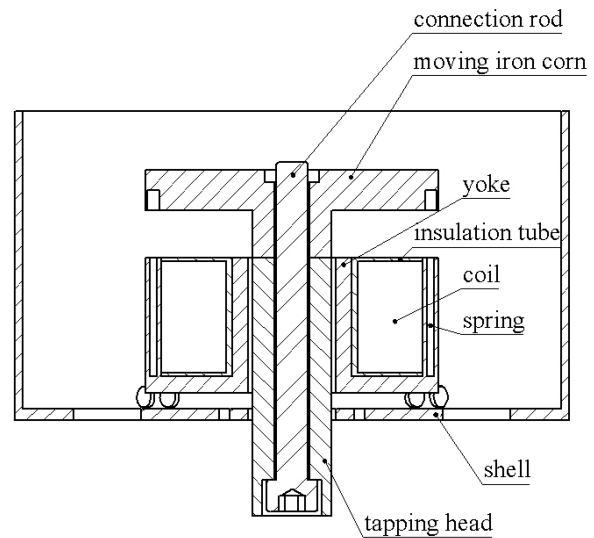insulation tube

coil

spring

shell

tapping head

Fig. 2. Massage head structure.

Ishii et al. [7] developed a 6 DOF facial tissue massage robotic system for oral disease and achieved a simple manipulator of bite tendons and other parts of the parotid gland. Luo and Chang [8] designed a multi-fingered robotic hand specifically for traditional Chinese medicine (TCM) massage operations and tested the massage effect. Moreover, some medical robots and surgical-assisted robots were developed to improve medical condition of rehabilitation [9,10]. On the one hand, simple massage equipment quickly spread into market due to low cost, but they are not widely accepted due to restricted massage function. On the other hand, the development of multi-function massage equipment is difficult due to its complex structure, difficulty in control and high cost. Therefore, this paper presents a novel massage robot with the features of portable structure, multi-function and high intelligence, and focuses on proposing an improved path planning algorithm to improve coverage rate and massage effect.

2. Structure design and model analysis

2.1. Structure of the massage robot

The structure of the presented wheeled massage robot is demonstrated in Fig. 1, which is mainly composed of tapping head, left and right driving wheels, front and rear driving wheels and sensors. The tapping head based on electromagnetic induction is mainly used to achieve tapping massage operation, and the driving wheels achieve rolling and kneading massage. Infrared distance sensors and crash sensors are placed around the wheeled massage robot (see Fig. 1) to detect environmental information of human back and achieve direction control of the massage robot.

In the previous work, tapping massage head (see Fig. 2) was designed and mounted on a mobile platform, which could change the massage area by moving the platform. During movement, the massage head should avoid touching human body to improve comfort. Therefore, a spring-based structure was design to balance the gravity of massage head. Massage head taps down with the action of springs, a yoke was added to increase the electromagnetic force which overcomes the spring force to achieve tapping operation.

The massage head works as follows: the winding coil is placed around the yoke, the movable core is magnetized when the coil is energized and it linearly moves under the action of the electromagnetic force. When the coil is powered off, the electromagnetic force disappears, the movable core return to the original position with the spring force. Tapping operation periodically takes place as the coil is periodically powered on.

2.2. Model analysis of the massage head

The model of robot massage head includes three parts, namely the electrical circuit, the magnetic circuit and the mechanics.

Windings and moving iron core part can be simplified as a resistance-inductance model. The driving voltage is

$$U = RI + \frac{d\Psi}{dt} = RI + \frac{d(LI)}{dt} \tag{1}$$

The equivalent inductance is

$$L = \frac{N^2}{R_m + R_\delta + R_l} \tag{2}$$

Where, R is the equivalent resistance, ψ is the flux generated by the coil in a magnetic field, N is the number of turns, R_m is the equivalent magnetic resistance, R_δ is the equivalent working air gap reluctance, R_l is the equivalent non-working air gap reluctance.

To simplify the calculation, we assume that the coil inductance L will not change during movement, then the Eq. (1) can be simplified as

$$u = Ri + L\frac{di}{dt} \tag{3}$$

To solve Eq. (3), the coil current of massage head could be calculated as

$$i = i_0 e^{-t/\tau} + \frac{U}{R}(1 - e^{-t/\tau}) \tag{4}$$

Where, $\tau = L/R$, i_0 is the initial current.

$$\begin{aligned} iN &= \Phi(R_m + R_\delta + R_l) \\ B &= \frac{iN}{AR_\delta} \\ R_\delta &= \frac{l_\delta}{\mu_0 A} \\ F_m &= \frac{\mu_0 i^2 N^2 A}{2(\delta - x)^2} \end{aligned} \tag{5}$$

Where, Φ is magnetic flux, A is the interaction area of the electromagnetic, δ is the initial distance, μ_0 is the air permeability, x is the displacement of the movable core, $0 \leqslant x \leqslant \delta$, F_m is the electromagnetic force of the moving iron core.

The magnetized moving iron core taps down with the action of electromagnetic force. It moves under the interaction of electromagnetic force, spring force and body back resistance. The motion equation is

$$m\frac{dv}{dt} = F_m - F_f - F_k \tag{6}$$

The differential equation of motion by combining Eqs (5) and (6) is

$$m\ddot{x} = \frac{\mu_0}{2} \cdot \frac{i^2 N^2 A}{(\delta - x)^2} - F_f - kx \tag{7}$$

Where, F_k is the spring load force, F_f is the back resistance.

The equations from Eqs (1) to (6) show the factors which affect the dynamic characteristics of the massage head.

3. Parameters design with orthogonal experiment method

3.1. Parameterization analysis

The orthogonal experiment method was used to analyze the sensitivity in this paper. Orthogonal experiment is the mathematical method which organizes and analyzes multi-factor scientifically [11]. In this paper, tapping intensity design scheme was made by orthogonal experiment method. Factors such as magnetic materials and the mass of massage head are generally pre-selected, so their influence on the electromagnetic force does not need to be analyzed. The main factors which affect the massage head pounding strength can be identified as:

Factor A, the coil turns N (turns);
Factor B, the coil current I (A);
Factor C, the distance between the iron core and the yoke d (mm).

To investigate the influence from the above factors, three levels (three values) were chosen for each factor, then there are totally 27 kinds of programs for the three chosen factors. However, it is not necessary to calculate all programs according to the aforementioned method. The maximum and minimum tapping force programs can be quickly and accurately determined by a few programs with the theory of orthogonal experiment method.

The number of turns can be determined between 2000 and 2200 turns depending on the size of the yoke and the coil. Accordingly, three levels of factor $A(A_1, A_2, A_3)$ were choose as 2000 turns, 2100 turns, 2200 turns respectively. With the previous simulation experience, the electromagnetic force is too small for the designed coil when the coil current is less than 0.30 A, the moving iron core springs rebound without touching the human back, which causes failing of massage function. The diameter of coil wire chosen in our work is 0.41 mm, the limit of coil current is 0.40 A when it works long time. Thus, the range of coil current should be controlled between 0.30 A and 0.40 A. As a result, three levels of factor $B(B_1, B_2, B_3)$ were chosen as 0.300 A, 0.325 A, 0.350 A respectively. When the robot is not working, the moving iron core needs to maintain a certain distance from the human back to avoid touching the back which may cause discomfort. However, too small electromagnetic force cannot overcome the spring resistance when the distance between the moving iron core and the back is more than 12 mm. Therefore, three levels of factor $C(C_1, C_2, C_3)$ were chosen as 10 mm, 11 mm, 12 mm respectively.

3.2. Analysis of orthogonal experiment

The finite element simulation method was used to calculate the initial electromagnetic force F_0 of these nine programs, and the results are listed in Table 1. For the electromagnetic force calculated in Table 1, we tried to determine which factor has more important influence on the electromagnetic force.

Table 1
Nine test programs by orthogonal experiment

Group	Programs	The initial electromagnetic force F_0/N
a	$A_1B_1C_1$	3.86
b	$A_2B_2C_2$	4.57
c	$A_3B_3C_3$	5.34
d	$A_1B_2C_3$	3.81
e	$A_2B_3C_1$	5.79
f	$A_3B_1C_2$	4.28
g	$A_1B_3C_2$	4.81
h	$A_2B_1C_3$	3.58
i	$A_3B_2C_1$	5.48

Table 2
Average and deviation of all these factors

Factors	Average			Total average	Deviation
A	A_1	A_2	A_3	4.61	0.0179
	4.16	4.65	5.03		
B	B_1	B_2	B_3	4.61	0.0461
	3.91	4.62	5.31		
C	C_1	C_2	C_3	4.61	0.0153
	5.04	4.55	4.24		

The influence extent of each factor on the design value was calculated by the difference of the calculated values at different levels, namely the difference between the average values is more, the influence is bigger.

Comparing the results shown in Table 2, it indicates that the deviation of factor B is much larger than factors A and C, which is 0.0461. So the coil current is the most important factor for electromagnetic force compared to the other two factors. Therefore, the number of turns and the distance between the moving iron core and the yoke could be determined based on the requirements of massage operation. Then, massage intensity could be controlled by adjusting the coil current value.

4. Path planning algorithm

4.1. Requirements of path planning

There are two massage paths based on the wheeled massage robot, tapping path and rolling/kneading path. Tapping path is the motion area of the tapping head of electromagnetic induction, rolling/kneading path is the motion area of the two driving wheels.

To get better massage effect, the requirements for path planning of massage robot were discussed and summarized as follows:

(1) Massage path must cover the entire massage area with high coverage rate;
(2) Be able to avoid all the obstacles and the edge of the human back;
(3) Walking path is composed of simple trajectory (straight line, arc);
(4) Path duplicate should be available.

4.2. The improved reciprocating path planning algorithm

The goal of complete coverage path planning is to make mobile robot efficiently move on the whole planned area and avoid obstacles, which requires the robot to traverse all the reachable area of human back area [12,13]. Massage path planning of the designed wheeled massage robot belongs to the range of typical complete coverage path planning. The TCM massage order generally cycles from top to bottom, and from inside to outside. Therefore, this paper chose reciprocating path planning algorithm to complete motion control of the massage robot.

The object of this study is a new wheeled massage robot which works on the human back, and it cannot be considered as a particle compared to the back area. For tapping massage path, only the middle
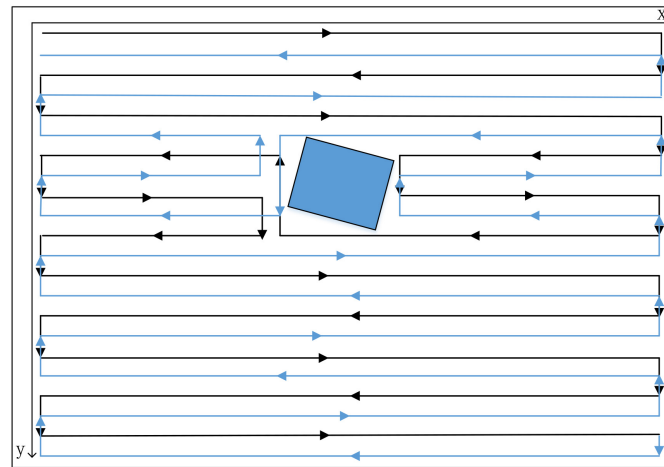
Fig. 3. Principle description of the improved reciprocating path planning algorithm.
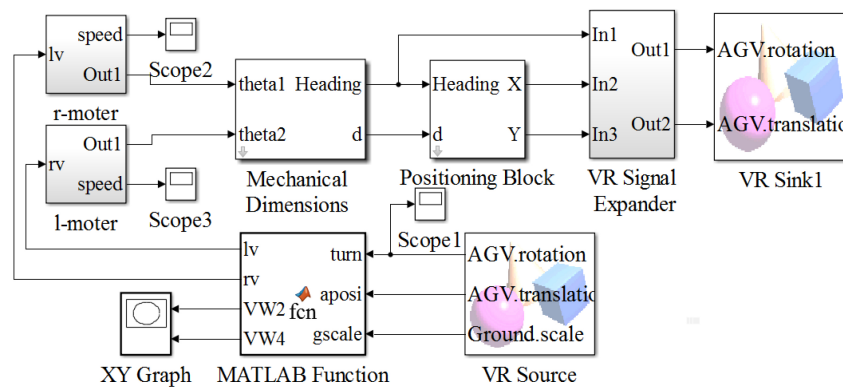

Fig. 4. Control system model of massage robot.

path of the massage area is valid. For rolling/kneading and other massage path, only the path of two wheels is valid. It can be calculated that the effective massage area is about one-third or two-thirds of the whole massage area when the massage robot moves along a circle. Therefore, this paper proposed the improved reciprocating path planning algorithm to improve regional coverage rate and massage effect.

The diagram of the improved reciprocating path planning algorithm is depicted in Fig. 3, the basic principle is described as follows: taking the reciprocating path planning algorithm as the foundation, the massage robot uses the infrared distance sensors and crash sensors to determine if there is a cliff (edge) or an obstacle during moving. When an obstacle or a cliff is detected, the massage robot immediately turns right 90°. Meanwhile, the A* algorithm was used to search the nearest uncovered area.

4.3. Modeling of control system

This paper established the control system model of the wheeled massage robot based on Simulink (see Fig. 4), it includes control subsystem of the motor, path algorithm control subsystem, parameter module of the massage robot and virtual reality interface module. The control signal is directly outputted to a
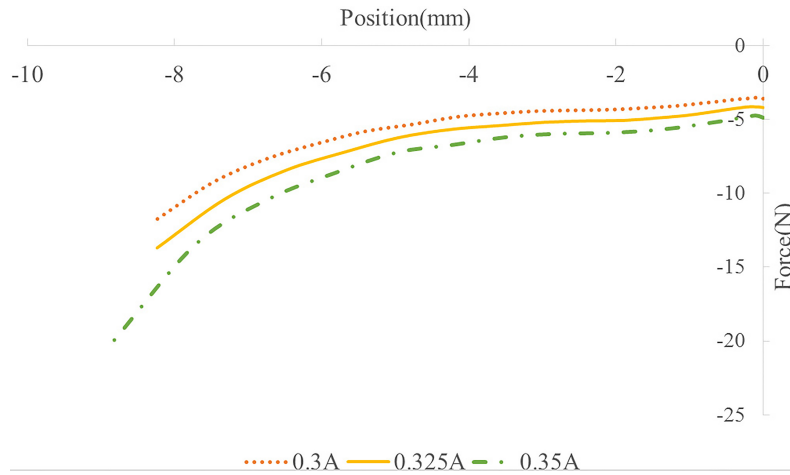
Fig. 5. Relationship between the electromagnetic force and the displacement of the moving iron core.

(a) t = 0.025 s
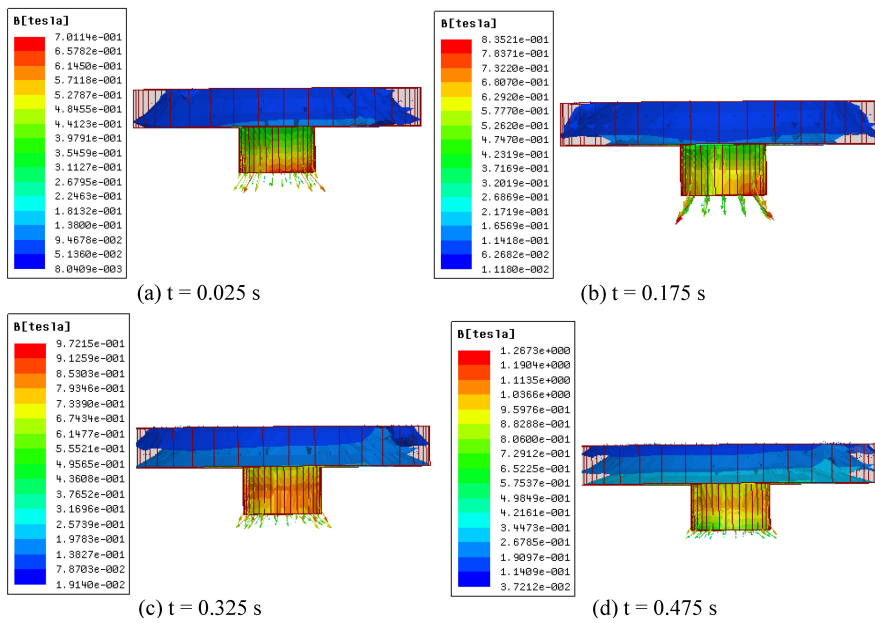
(b) t = 0.175 s

(c) t = 0.325 s

(d) t = 0.475 s

Fig. 6. Vector distributions of magnetic induction B of the moving iron core at different time.

virtual operating environment by virtual reality (VR) Sink block, and the operation of the massage robot could be observed through a browser window.

5. Results

5.1. Structure optimism of massage head

Considering factors like massage comfort and electromagnetic force, the distance between moving iron core and the yoke was chosen as 12 mm. the massage percussion depth is about 4 mm according
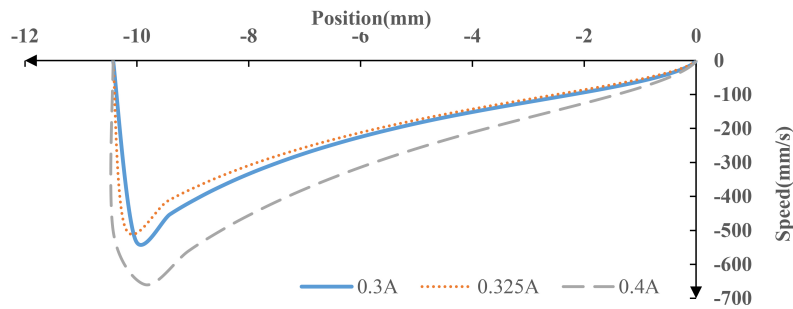
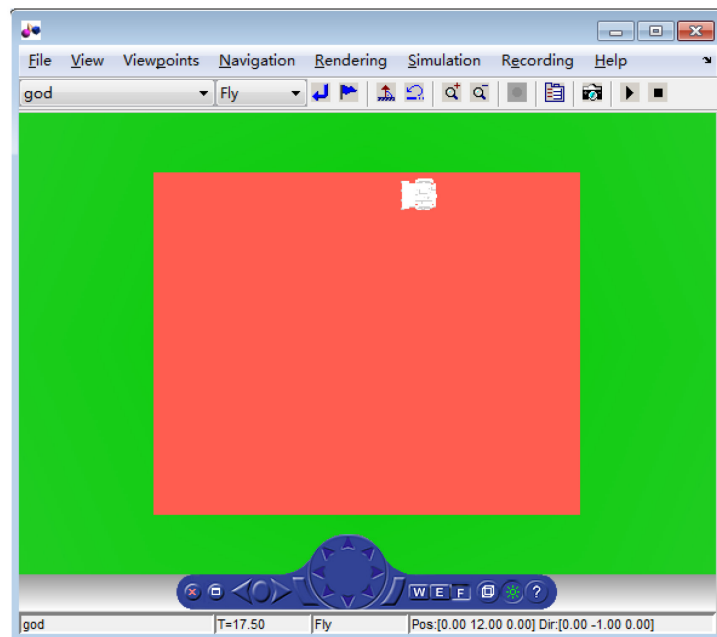Fig. 7. Relationship between velocity and displacement of the moving iron core.

Fig. 8. Visual interface of massage robot movement.

to TCM massage and the maximum movement stroke of the moving iron core is 8 mm. Considering factors like the size of the yoke and coil diameter, the number of coil turns was chosen as 2100. The relationship between the electromagnetic force and displacement of moving iron core under the current of 0.3 A, 0.325 A, 0.35 A are given in Fig. 5. It shows that massage force varies from 10 N to 20 N. Tapping intensity usually varies between 10 N and 30 N according to TCM massage theory. It indicates that all the chosen current values satisfy the requirements.

When the coil current is 0.35 A, the vector distributions of magnetic flux density B of the moving iron core are illustrated in Fig. 6. It indicates that the distance between the moving iron core and the yoke gradually reduces with time but the magnetic flux density gradually increases.

5.2. Control of massage intensity

From the simulation results, it can be inferred that the coil current is the most important factor which affects massage intensity based on orthogonal experiment. Compared to other factors, the coil current
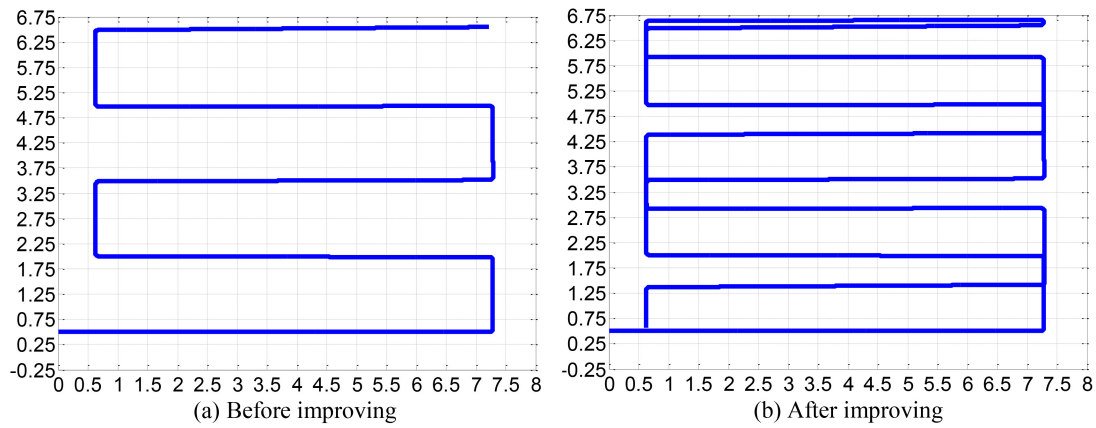
(a) Before improving

(b) After improving

Fig. 9. Comparison before and after improving of tapping path.

(a) Algorithm before improving

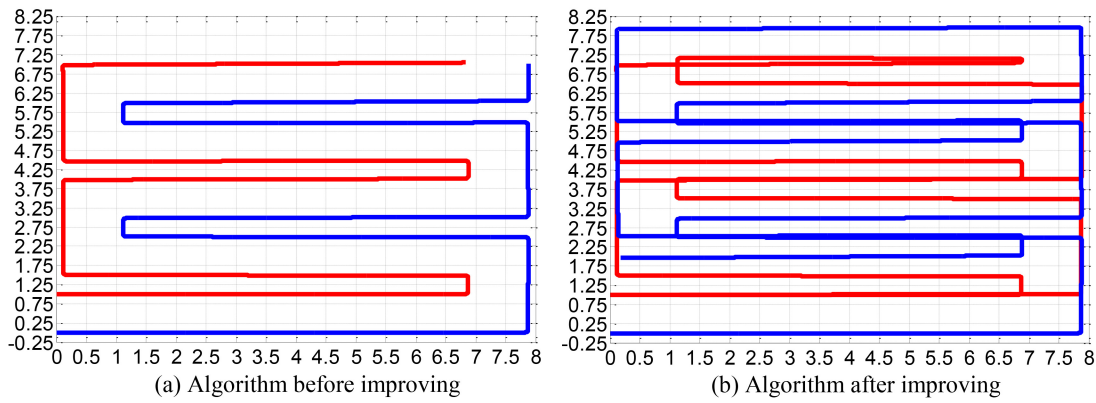(b) Algorithm after improving

Fig. 10. Comparison before and after improving of rolling/kneading path.

is more flexible to control the massage intensity. The relationship between velocity and displacement of the moving iron core with the coil current 0.3 A, 0.35 A and 0.4 A are illustrated in Fig. 7. The electromagnetic forces are between $10 \sim 20$ N at the initial time for all three current values. It was found that the electromagnetic force is too small when the coil current is less than 0.30 A, the moving iron core was bounced back without touching the human back due to the spring force. Coil diameter was chosen as 0.41 mm, and the operating current should not exceed 0.4 A if it works long time. Thus the coil current must fluctuate between 0.3 A and 0.4 A to guarantee the safety of the device and massage comfort. Different massage intensity and tapping rate can be produced by adjusting the coil currents to achieve different massage effect ultimately.

5.3. Simulation of path planning

The actual movement of the massage robot in virtual operating environment can be observed after completing the above modeling work (see Fig. 8). The simulation results of the proposed algorithm before and after improving tapping path are presented in Fig. 9. It can be calculated that the coverage rate is only 35.27% by using the traditional reciprocating path planning algorithm, while the coverage rate reaches up to 60.27% with the improved reciprocating path planning algorithm.

For rolling/kneading path, the corresponding results are shown in Fig. 10. It can be seen that the coverage rate is only 58.82% using the traditional reciprocating path planning algorithm as shown in Fig. 10a, it is improved to 84.93% using the improved reciprocating path planning algorithm as shown in Fig. 10b.

6. Discussion

It's very difficult for the current massage devices to give friendly interaction to people, especially the aged. A massage robot could reproduce the expert operations with individualized manipulation parameters and enhanced safety control strategies. Thereby, our team made efforts to provide a portable massage robot with tapping, rolling and kneading operations [14]. In order to promote the experience and skills of experts and reduce labor intensity during massage, massage robotic systems were proposed to perform massage operations instead of experts. However, most of the existing massage devices could complete restricted operation and the whole massage process was not completely considered. By comparison, the massage robot presented in our work could perform three kinds of operations. Nevertheless, the treatment effect of the massage robot needs to be assessed clinically, and the structure may be improved to provide more operations.

With the above analysis, it is known that the practical moving area of massage robot is not the effective massage area. Therefore, this paper took the right wheel of massage robot as the analysis objects and respectively used reciprocating path planning algorithm and the improved reciprocating path planning algorithm to simulate massage path. The simulation results are presented in Section 4. The coverage rate was calculated as: Coverage rate = The covered grids/All grids, it is an important indicator to measure the effectiveness of the complete coverage path planning algorithm. The calculated coverage rate indicates that the improved reciprocating path planning algorithm proposed in this paper can greatly improve coverage rate, and then the massage effect gets improved.

The simulation results of the proposed improved algorithm were compared to the traditional algorithm with tapping and rolling/kneading path. To further study the improvement and the feasibility of the proposed algorithm, the Angle-Time and Speed-Time results were obtained, and the flexibility of the wheels has be proven. The control strategy of the whole system would be optimized for the balance and stability in the future work.

7. Conclusions

This paper proposed the improved reciprocating path planning algorithm for the autonomous mobile massage robot which was designed based on the principle of electromagnetic induction, and established the control system model by using Matlab/Simulink platform. The influence caused by coil current, coil turns and the distance between the moving iron core and the yoke on massage intensity were figured out with a simplified model. The coil current was found to be the most important factor on electromagnetic force by orthogonal experimental method. According to the simulation results and the experience of massage operations, the number of turns and the distance between the moving iron core and the yoke were determined prior to coil current to optimize the structure parameters of massage head, and it is feasible to control the massage intensity by adjusting the value of coil current. Furthermore, the traditional and improved reciprocating path planning algorithm were simulated and analyzed for three different

massage operations. It can be concluded that the proposed algorithm is suitable for massage environment without the need of establishing unknown environmental model, the control tests also show that the proposed algorithm can effectively improve coverage rate, and the massage effect accordingly gets improved.

Acknowledgments

Conflict of interest

None to report.

References

[1] Kamali F, Panahi F, Ebrahimi S, Abbasi L. Comparison between massage and routine physical therapy in women with sub acute and chronic nonspecific low back pain. J Back Musculoskelet. 2014, 27(4): 475-480.

[2] Huang Y, Li J, Huang Q, Soueres P. Anthropomorphic robotic arm with integrated elastic joints for TCM remedial massage. Robotica. 2015, 33(2): 348-365.

[3] Wang W, Shi Y, Yang N, Yuan X. Experimental analysis of drilling process in cortical bone. Med Eng Phys. 2014, 36(2): 261-266.

[4] Wang W, Shi Y, Goldenberg AA, Yuan X, Zhang P, He L, et al. Experimental analysis of robot-assisted needle insertion into porcine liver. Biomed Mater Eng. 2015, 26: S375-380.

[5] Ishii H, Koga H, Obokawa Y, Solis J, Takanishi A, Katsumata A. Path generator control system and virtual compliance calculator for maxillofacial massage robots. International Journal of Computer Assisted Radiology and Surgery. 2010, 5(1): 77-84.

[6] Fazeli M, Pourrahmat M, Liu M, Guan L, Collet J. The Effect of Head Massage on the Regulation of the Cardiac Autonomic Nervous System: A Pilot Randomized Crossover Trial. J Altern Complement Med. 2016, 22(1): 75-80.

[7] Ishii H, Koga H, Obokawa Y, Solis J, Takanishi A, Katsumata A. Development and experimental evaluation of oral rehabilitation robot that provides maxillofacial massage to patients with oral disorders. Int J Robot Res. 2009, 28(9): 1228-1239.

[8] Luo R, Chang C. Electromyographic Evaluation of Therapeutic Massage Effect Using Multi-finger Robot Hand. 2011 Ieee International Conference on Robotics and Automation. IEEE International Conference on Robotics and Automation ICRA2011. p. 2431-2436.

[9] Wang W, Zhang P, Shi Y, Jiang Q, Zou Y. Design and compatibility evaluation of magnetic resonance imaging-guided needle insertion system. Journal of Medical Imaging and Health Informatics. 2015, 5(8): 1963-1967.

[10] Wang W, Shi Y, Yuan X, Su S. Design and analysis of magnetic resonance compatibility of ultrasonic motor in surgical robot. Xibei Gongye Daxue Xuebao/Journal of Northwestern Polytechnical University. 2014, 32(1): 147-151.

[11] Yuan J, Zhou J, Yu C, Wang Y, Chen B, Song M, et al. Study on harmonics characteristics of magnetic-valve controllable reactor based on the finite element method. Ieee T Magn. 2015, 51(3).

[12] Hu L, Wang Y, Zhang J, Zhang J, Cui Y, Ma L, et al. A massage robot based on Chinese massage therapy. Industrial Robot. 2013, 40(2): 158-172.

[13] Gao H, Lu S, Wang T, Liu C, Kang B, Ji Y, et al. Research and development of Chinese medical massage robot. Jiqiren/Robot. 2011, 33(5): 553-562.

[14] Wang W, He L, Jiang Q, Zhang P, Shi Y. Path Planning Algorithm of a Novel Massage Robot. 9th; International Congress on Image and Signal Processing, BioMedical Engineering and Informatics (CISP-BMEI). 2016, 1690-1694.